

The effect of the starting powders particle size on the electrical properties of sintered Co doped ZnO varistors

S. Hamdelou · K. Guergouri · L. Arab

Received: 8 September 2014 / Accepted: 13 November 2014 / Published online: 23 November 2014
© The Author(s) 2014. This article is published with open access at Springerlink.com

Abstract Pure and Co doped zinc oxide nanopowders have been synthesized by sol–gel route. The obtained powders, after calcination in air at 550, 650, 750 and 850 °C, were consolidated and sintered using microwaves. The effect of sintering temperature on the density and electrical properties was investigated. The best characteristics are obtained using a sintering temperature equal to 1,075 °C. The powders and sintered samples are characterized by X-ray diffraction, microstructure images, density and electrical measurements. The studied nanopowders have: a density of 5.22 (g/cm³), a breakdown voltage of 446.5 V/mm and a coefficient of non-linearity of 11.48 for ZnO doped with 7 mol% Co, and a density of 5.19 (g/cm³), a breakdown voltage of 292.5 V/mm and a non-linearity coefficient of 11.62 for ZnO doped with 5 mol% Co. The XRD results indicate that pure and Co doped ZnO powders are solid solutions crystallizing in pure würtzite structure, and consisted of a mixture of nanoparticles with an average grain size between 36 and 210 nm. The grain size decreases with increasing Co concentration and reaches its lowest value at 7 mol% Co and increases with increasing temperature. On the other hand the increase of Co concentration leads to a decrease of the porosity and an

increase of the density of samples sintered at 1,070 °C and leads also to an increase of the electric field (E) in the non-linear area. The samples of 5 mol% Co sintered at 1,075 °C, show that the non-linear coefficient α decreases by increasing of calcined temperature, therefore increases with decreasing of grain and particle sizes.

Keywords Co doped ZnO · Grain size · Varistor · Electrical properties · Microwave · Porosity · Density

Introduction

Due to their non-linear electrical coefficient or varistor properties, pure and doped ZnO materials attract more and more attention of researchers and industrials (Matsuoka et al. 1969; Subasri et al. 2009).

Such materials are usually used to manufacture devices used for the protection of electrical circuits and electronic devices against voltage surge (Subasri et al. 2009). ZnO is also, widely used in various fields such as piezoelectricity, electronics, optics, photovoltaic, thermal and spintronics (Wood and Austin 1975; Monteiro et al. 2003).

The challenge now is to improve the characteristics of these materials. This is what has led many researchers to study these materials in their nanoscale form on one hand and doping with specific elements on the other hand.

Among several methods of ZnO nanopowder elaboration, the sol–gel is a widely used one; it is a simple method with a low cost on one hand, and a good quality of the obtained powder at room temperature on the other hand. That is why we used this method as a means of synthesizing our powders (Arab et al. 2012; Miao et al. 1996).

Doping ZnO with various elements such as Co and Mn or some oxides such as Bi₂O₃, Pr₆O₁₁, Sb₂O, CoO, MnO,

S. Hamdelou
Laboratory of Physics and Chemistry of Semiconductors,
University Constantine 1, 25000 Constantine, Algeria

K. Guergouri (✉)
Physics Department, Faculty of Exact Sciences, University Larbi
Ben M'Hidi, 04000 Algeria, Oum El Bouaghi, Algeria
e-mail: kamelguergouri@yahoo.com

L. Arab
Materials and Semi Materials Laboratory, University Mohamed
Kheider, 07000 Biskra, Algeria

Cr_2O_3 leads to expand the use of this material to other fields or to improve its performance such as varistor characteristics.

It is important to report that some of these dopants such as Bi_2O_3 , Sb_2O_3 and Pr_6O_{11} interact generating secondary intergranular phases, while others, such as Co and Mn, pass into solution in ZnO grains (Lin et al. 2007).

Furthermore, much work have been done in electrical properties of ZnO varistors; it is demonstrated that these properties are greatly dependent on the material composition (nature and amount of doping) (Savary et al. 2011a), density of sintered samples (Nahm 2003), grains size (Anas et al. 2012), morphology and distribution of the second phases. It is reported also that the double Schottky barrier formed between two ZnO grains is responsible for the non-

ohmic behavior of varistors (Peng et al. 2010; Blatter and Greuter 1986). Besides this Duran et al. (2003) had reported that the breakdown voltage of varistors increased with decrease in grain size and improved with density and doping elements distribution homogeneity.

Although these investigations, there are few works that have either been carried out on systematic study of the effect of cobalt on ZnO varistor effect, using nanocrystalline powders as starting materials, or preventing the grain growth, as much as possible, during the sintering process, which is the aim of this study.

To do this, Co doped ZnO nanopowders were synthesized by means of sol–gel route, and then sintered, as pellets, in microwave sintering, which has the advantage of reducing the grain size and to have dense materials, using a very short time of sintering (Subasri et al. 2009; Savary et al. 2011a).

It is well-established that the addition of cobalt oxides in the matrix of ZnO improves the non-linear properties (Onreabroy et al. 2006; Long et al. 2010; Nahm and Kim 2002; Onreabroy and Sirikulrat 2006). Onreabroy et al. (2006) found that, the ZnO–CoO-based varistor, with an average grain size of 16 μm , have an ohmic behavior at low sintering temperatures (below 1,000 $^\circ\text{C}$), and also at high sintering temperatures (above 1,100 $^\circ\text{C}$). However, at intermediate sintering temperatures (1,000–1,100 $^\circ\text{C}$),

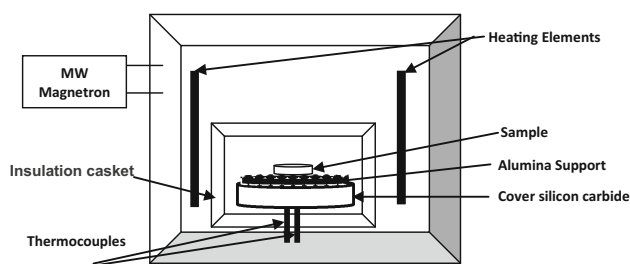


Fig. 1 Microwave sintering furnace

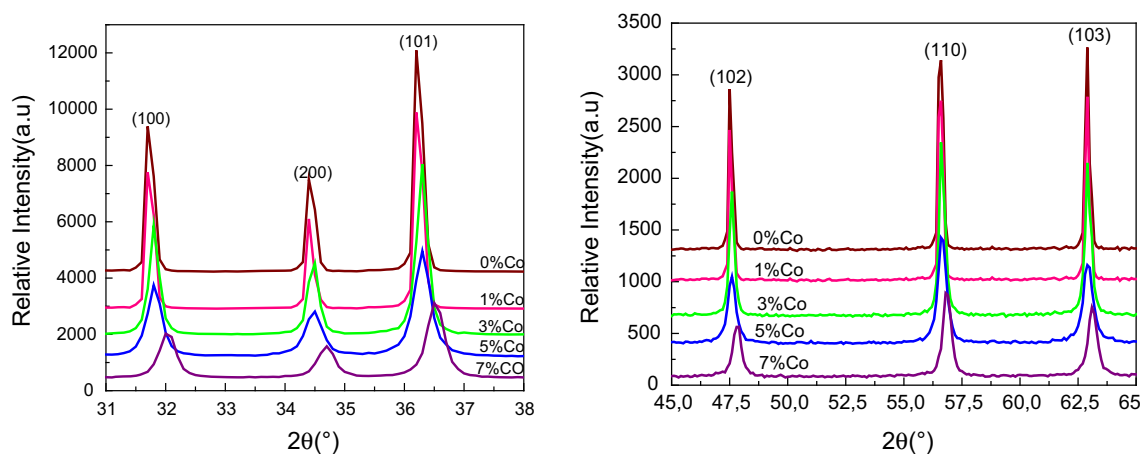


Fig. 2 XRD patterns of pure and Co doped ZnO nanopowders

Table 1 Effect of Co concentration on properties of Co doped ZnO varistors

Co content (mol%)	D (powders) (nm)	D (SEM) (μm)	Density (g/cm^3)	Porosity (%)	V_b (V/mm)	V_{gb} (v)	α
0	210	–	5.32	–	71	–	5.38
1	155	6.10	4.95	10	99	0.603	6.75
3	118	2.81	5.02	6.68	223	0.627	8.95
5	67	2.03	5.19	4.66	292.5	0.593	11.62
7	36	1.75	5.22	3.88	446.5	0.781	11.48

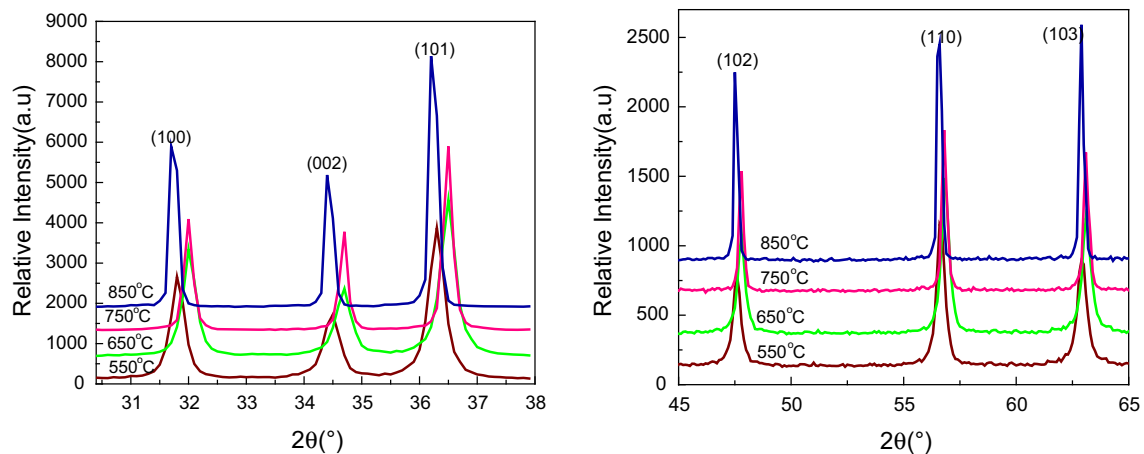


Fig. 3 X-ray diffraction patterns of 5 % Co doped ZnO nanopowders as a function of calcination temperature

Table 2 Effect of calcination temperature on characteristics of 5 % mol Co doped ZnO nanopowders

Calcination temperature (°C)	<i>D</i> (powders) (nm)	<i>D</i> (SEM) (μm)	Density (g/cm ³)	Porosity (%)	<i>V_b</i> (v/mm)	<i>V_{gb}</i>	α
550	67	2.03	5.19	4.66	292.5	0.593	11.62
650	89	2.60	5.04	7.11	228	0.592	9.38
750	125	4.37	4.75	11.58	134	0.585	6.92
850	168	–	4.32	–	92.2	–	5.80

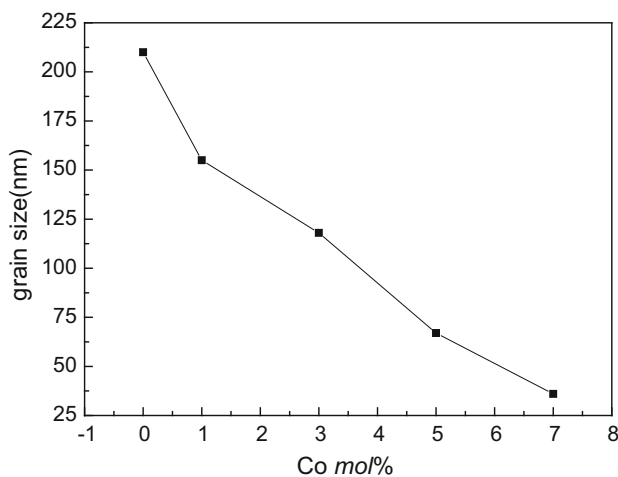


Fig. 4 ZnO nanopowders grain size as a function of Co concentration

the ZnO–CoO-based varistors show a non-ohmic behavior. Unfortunately, they did not calculate the values of the non-linearity coefficient α , which has been investigated in this study.

Several studies (Subasri et al. 2009; Long et al. 2010; Cheng et al. 2012; Anas et al. 2010) have investigated the properties of ZnO, doped with different elements-based varistors using various methods, but few works have been

devoted to study the properties of ZnO–CoO-based varistors, especially, using the microwave sintering on one hand and to use nanocrystalline powders for manufacturing pellets used for this study on the other hand; it is what gives this study its originality, in which we investigated the influence of grain size and amount of Co on the properties of ZnO–CoO-based varistors.

To do this we synthesized nanopowders, using the sol-gel route.

The obtained powders have been characterized by X-ray diffraction (XRD) and scanning electron microscopy (SEM). Then the nanopowders were pressed by disks with diameter of 15 mm under pressure of 75 MPa and then sintered by microwave. The current–voltage *I*(*V*) behavior was measured using a direct current power supply (1,500 V, 10^{−2} A), a Nano-Ampere meter and a Voltmeter. The density and the non-linearity coefficient α of different samples were then calculated.

Experimental

Synthesis

Co-doped ZnO nanopowders with Co varying from 0 to 7 mol% were synthesized by the sol-gel technique.

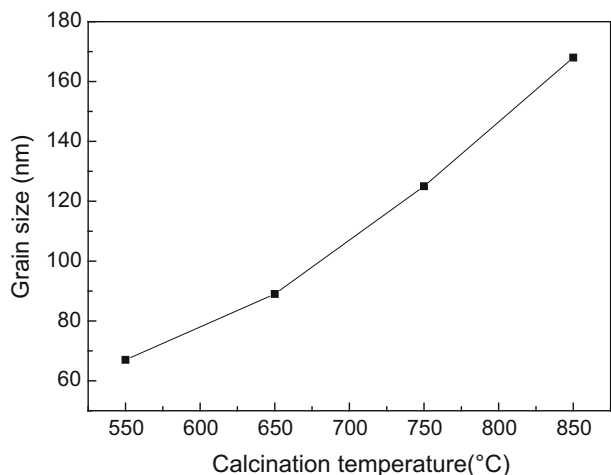


Fig. 5 Variation of the grain size of 5 % mol Co doped ZnO nanopowder as a function of calcination temperature

The reagents used are: Zinc acetate dehydrate [Zn(CH₃COO)₂·2H₂O: purity >99 %, Biochem–Chempharma], Cobalt acetate tetrahydrate [Co(CH₃COO)₂·4H₂O: purity >99 %, Biochem–Chempharma], Lactic acid and Ethanol.

First, the zinc acetate dehydrate and cobalt acetate tetrahydrate are dissolved in ethanol, and then the obtained solution is stirred at 70 °C for 2 h. After that, the lactic acid is dripped into the obtained mixture until obtaining

transparent and homogeneous solution. The molar ratio of ethanol to lactic acid is 3. The final solution was then dried at 100 °C for 1 h and calcined in air at 550 °C for 2 h. Finally, a kind of a green nanopowder is obtained.

Sintering

Microwave sintering was carried out in a 2.45 GHz, 850 W microwave furnace (model LG-MC-805AY, South Korea (Fig. 1)). The thermocouple is connected to a circular disk (thickness = 2 cm and diameter = 3 cm) of SiC, which is placed on an alumina support to avoid a probable contamination. On this support is placed the sample to be sintered. The whole is placed in an insulating chamber made of alumina fibers.

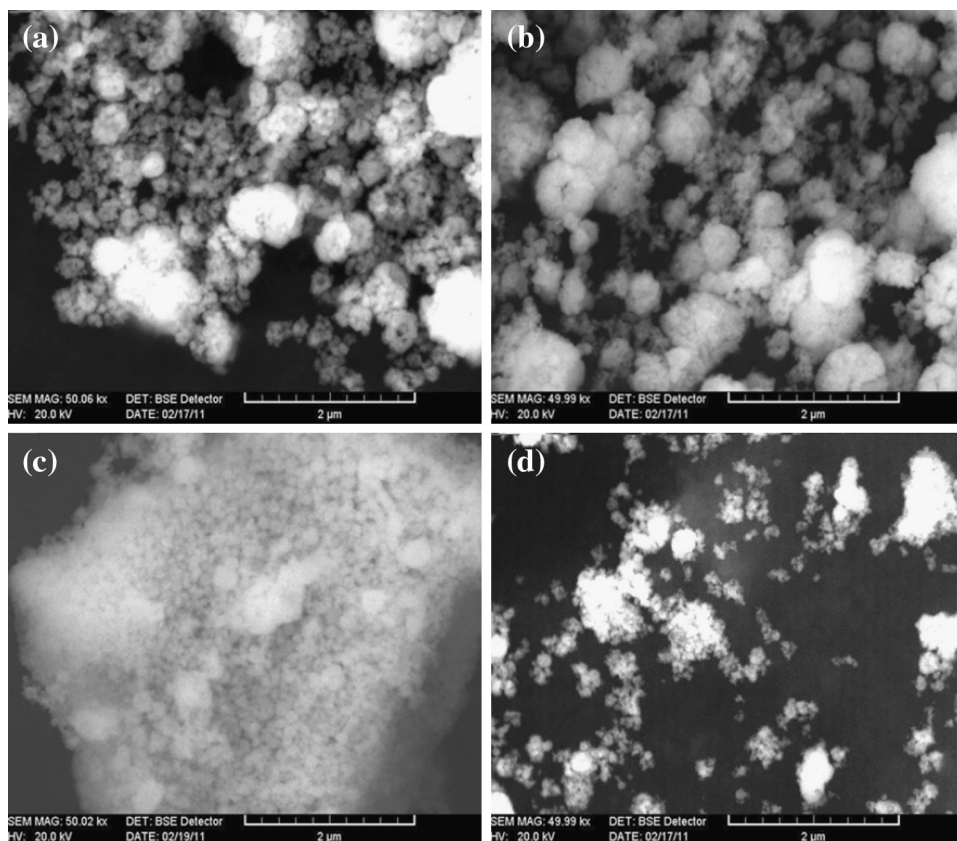
After closing the oven, the following parameters are defined: the sintering temperature given by the thermocouple attached to the magnetron, the sintering time and the chosen power.

Investigations were carried out in air using one chosen sintering temperature.

Characterization

The nanopowders structure was identified by XRD using the CuK_α ($\lambda = 0.154056$ nm) radiation of a BRUKER

Fig. 6 SEM images of Co doped ZnO nanopowders: **a** 1 mol% Co calcined at 550 °C, **b** 5 mol% Co calcined at 550 °C, **c** 7 mol% Co calcined at 550 °C, **d** 5 mol% Co calcined at 650 °C



AXS, D8 advance X-ray diffractometer. The density of the sintered samples was measured by means of Archimedes method using a SCALTEC SBC22 analytical weighing balance.

The particle size of the synthesized powders, before and after sintering, their morphology are determined by means of a VEGA TS 5,130 MM, TESCAN scanning electron microscope (SEM).

The average particle size (D) of sintered samples is determined by the lineal intercept method, given by the following equation:

$$D = 1.56 L/MN,$$

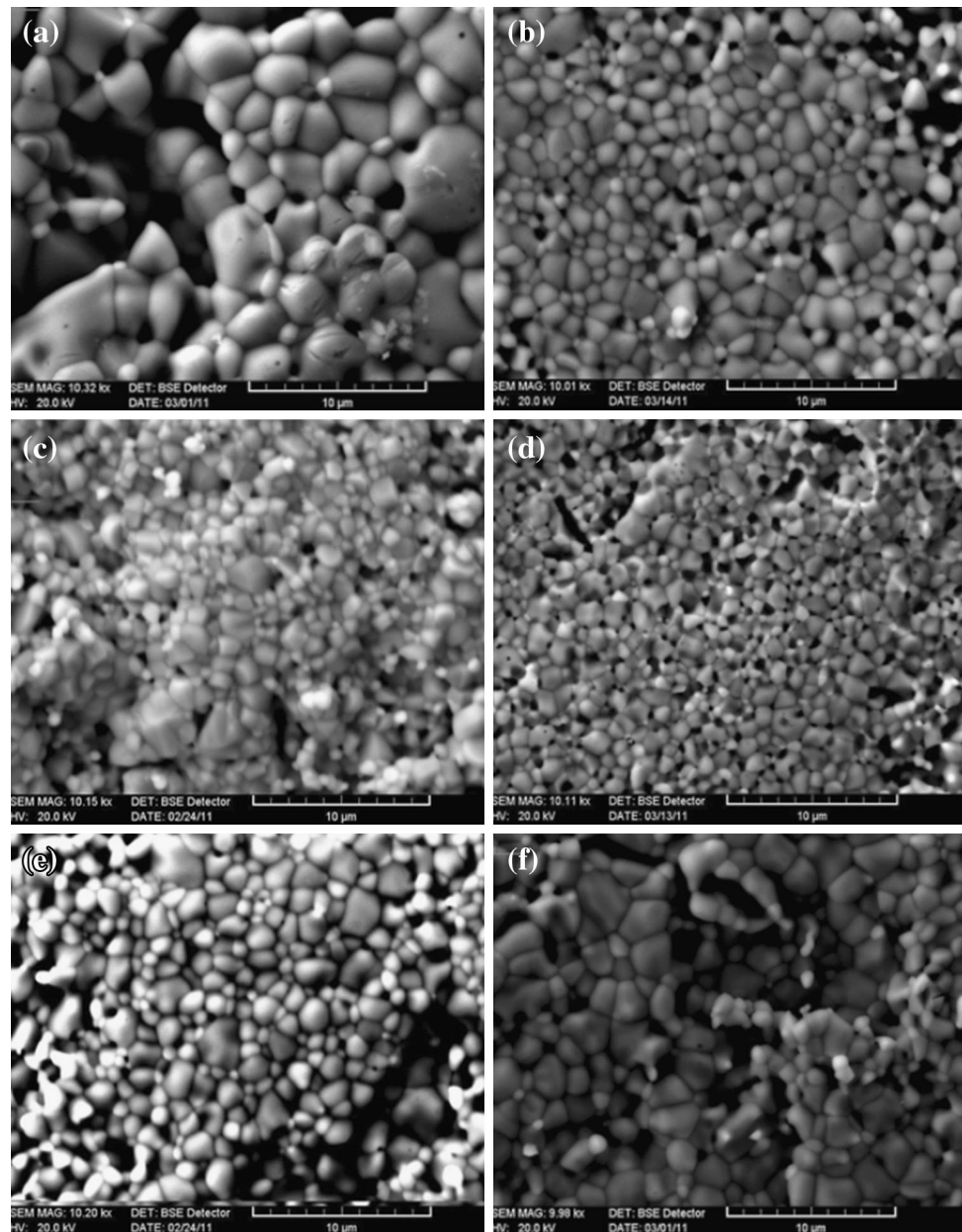
where L is the random line length on the micrograph, M the magnification of the micrograph and N the number of grain boundaries intercepted by the lines (Nahm et al. 2004; Wurst and Nelson 1972).

However, the average of the grain size of the powders is calculated by the Scherer's equation (Ait Ahcen et al. 2006):

$$d = \frac{0.9 \lambda}{\Delta\theta \cos\theta}$$

where d is the grain size, λ the X-ray wave length ($\lambda = 1.5418\text{\AA}$), $\Delta\theta$ the full width at half-maximum (FWHM) and θ the Bragg angle.

Fig. 7 SEM images of sintered samples at 1,075 °C: samples calcined at 550 °C: **a** 1 mol% Co, **b** 3 mol% Co, **c** 5 mol% Co, **d** 7 mol% Co. **e** 5 mol% Co calcined at 650 °C and **f** 5 mol% Co calcined at 750 °C



Finally, the current–voltage I (V) characteristics are measured using a direct current power supply (1,500 V, 10^{-2} A), a Nano-Ampere meter and a Voltmeter. The sintered samples are covered by silver paste and heated at 600 °C for 30 min. The nonlinear exponent (α) is calculated from the empirical relation: $J = KE^\alpha$ (Onreabroy et al. 2006), where K is a constant, J and E the current density and electric field, respectively. α is given by: $\alpha = (\log J_2 - \log J_1)/(\log E_2 - \log E_1)$ (Levinson and Philipp 1975), with: $J_1 = 0.1$ mA, $J_2 = 1$ mA, E_1 and E_2 are the electric fields corresponding to J_1 and J_2 , respectively.

Results and discussion

Figure 2 shows XRD patterns of pure and Co doped ZnO nanopowders synthesized by sol–gel technique. The spectra exhibit peaks of the wurtzite structure, and there are no additional peaks after Co doping, indicating that we have a solid solution for all Co concentrations.

One of intermediate values (Table 1) is obtained with the 5 % mol Co doped ZnO powder. This is why this powder has been chosen for the study as a function of the calcination temperature. The results of the XRD patterns are presented in Fig. 3.

The influence of the Co concentration of the varistors made of Co doped ZnO nanopowder on the structural, morphological and electrical properties is shown in Tables 1 and 2.

The grain size of Co doped ZnO nanopowders decreases by increasing Co concentration as it is shown in Fig. 4, and it reaches its lowest value at nearly 36 nm for 7 % mol% Co.

With regard to the calcination temperature (Fig. 5), it is noticed that the grain size increases with increasing temperature; the values vary from 67 to 168 nm. These results can be connected to the particle size variation, as it is seen in SEM images (Figs. 6, 7), which show that the particle size decreases when Co concentration increases and increases when the calcination temperature increases. Finally, we can say that the grain size and the particle size vary in the same way.

SEM images of Co doped ZnO samples, for different amount of Co, calcined at different temperatures are shown in Fig. 7. All samples have a morphology consisting of particles, uniformly distributed, in the presence of pores, whose number or the porosity of the sample decreases when the concentration of Co increases (Table 1) and increases when the calcination temperature increases (Table 2), which is easily connected to the variations of the grain and particles size. They all vary in the same way.

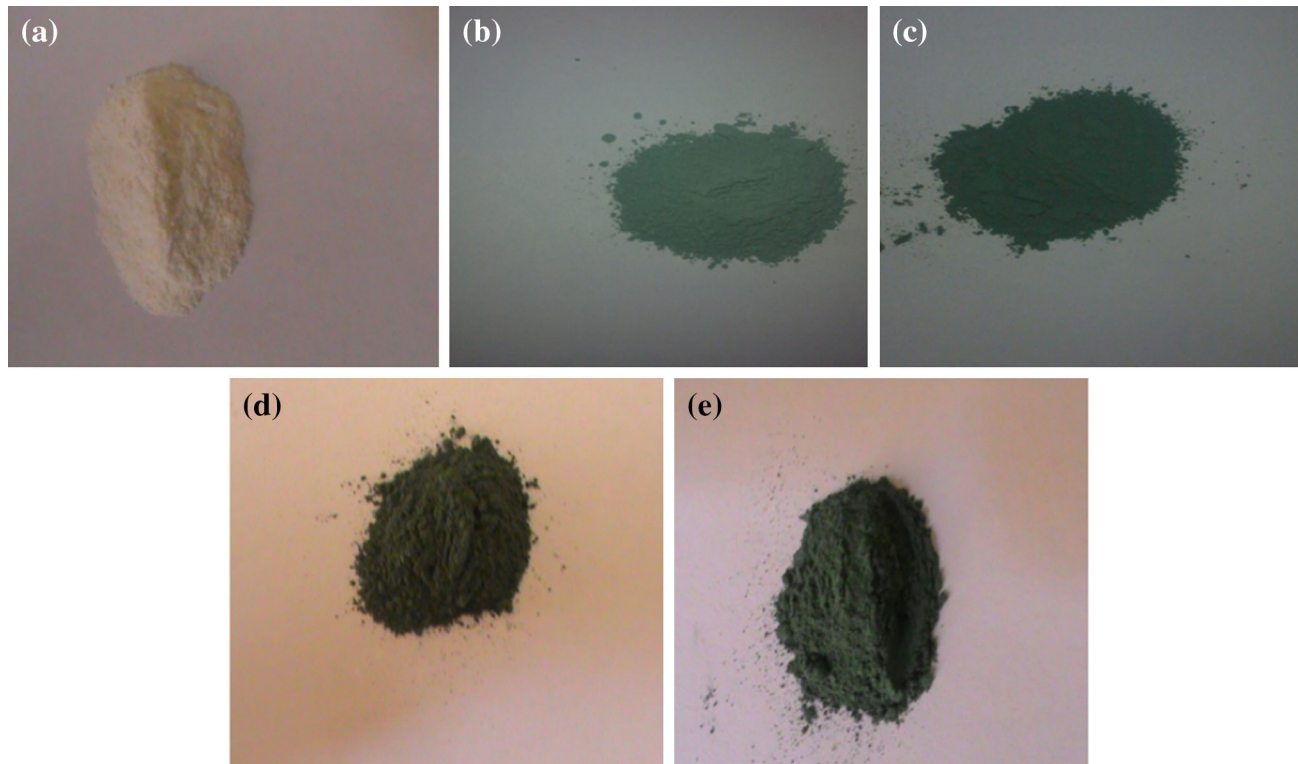


Fig. 8 Appearance of powders: **a** commercial pure ZnO powder, **b–e** green powders prepared by sol–gel, **b** 1 % Co, **c** 3 % Co, **d** 5 % Co, **e** 7 %Co

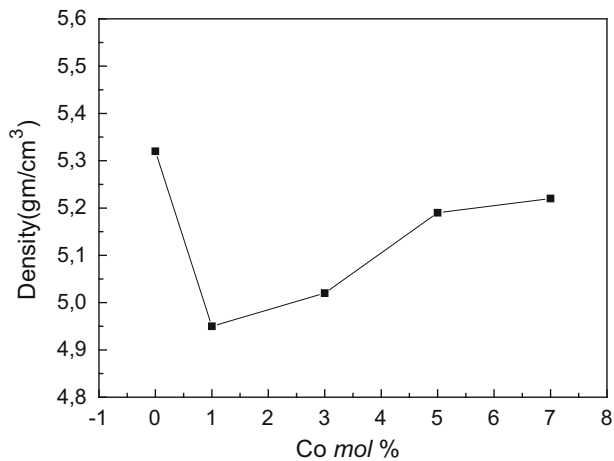


Fig. 9 Density of samples sintered at 1,075 °C as a function of Co concentration

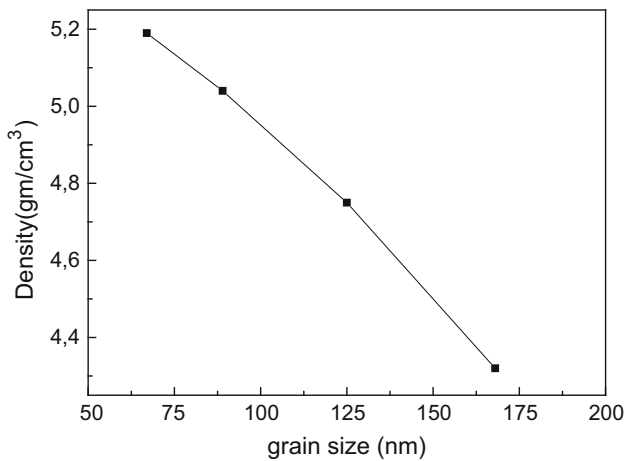


Fig. 10 Density of samples sintered at 1,075 °C as a function of the grain size

We can also deduce, from SEM images (Fig. 7), that the rearrangement is achieved more easily for small particles than for larger ones.

Additionally, we observe no second phases between particles, which confirm, once again, that Co atoms pass into solution in ZnO matrix.

Another important result is related to the color of the powders. Figure 8 shows also that the green color becomes darker when the Co concentration increases. The obtained green powders (Fig. 8) consist in particles agglomerated together, which could be easily broken down during pelleting and then used to obtain green pellets uniformly packed.

The calculation of the density of samples sintered at 1,075 °C has confirmed the previous results, since it has been recorded that the density increases with increasing Co concentration (Table 1) and decreases by increasing calcination temperature, as shown in Table 2 for 5 % mol Co doped ZnO, which can also be seen in Figs. 9 and 10, respectively.

For a more complete study, the investigation of the influence of sintering time is recommended. It was not done in this work but it will undoubtedly be the subject of future investigations.

Figure 11 shows the variation, at room temperature, of the electric field as a function of the current density [$E(J)$] for all samples. The curve can be divided into two regions: the first one (the ohmic region) is known as a high resistance region and the second one (the non-ohmic region) is known as a very low resistance region.

The non-linear electrical behavior given by the coefficient α is due to solid state reactions and formation of potential barriers between grains (Mirzayi and Hekmatshoar 2013). More the curve is pronounced more α is great.

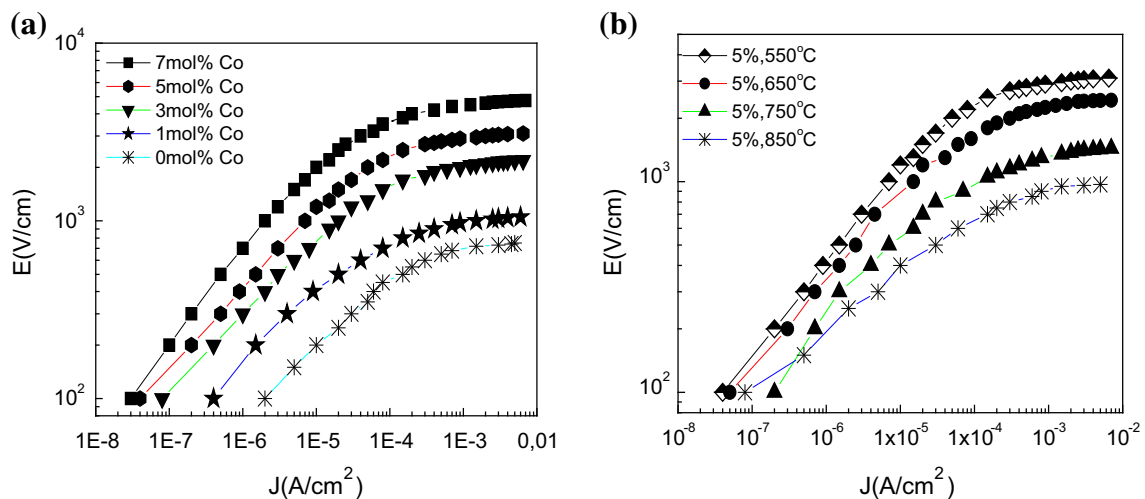


Fig. 11 $E(J)$ characteristics of varistors: **a** as a function of Co amount, **b** as a function of the calcination temperature

The obtained results show that the voltage (electric field E) in the non-linear area increases by increasing Co concentration, thus E increases with decreasing of grain and particle sizes. But the current density is reduced, particularly for the 5 mol% Co samples calcined at different temperatures. This does not prevent the non-linear coefficient α to increase with increasing Co concentration up to 11.62 for 5 mol% Co. We notice, however, that the values for 5 and 7 mol% Co are very close.

The samples of 5 mol% Co sintered at 1,075 °C, show that the non-linear coefficient α decreases by increasing of calcined temperature, therefore increases with decreasing of grain and particle sizes.

Other studies showed that the Co doped ZnO, which particle size is about 16 μm , exhibits a non-linear behavior in the sintering temperature interval [1,000, 1,100 °C].

It is good to remember that the breakdown electric field E_B is the field related to the current flowing through the varistor and is equal to 1 mA/cm² (Sedky et al. 2012; Nahm 2012; Hembram et al. 2011).

The different values of E_B can be deduced from curves of Fig. 11. They allowed to calculate the breakdown voltage per grain boundary (V_{gb}), given by the equation (Anas et al. 2010): $E_B = V_{gb}/d$ and listed in Tables 1 and 2, d being the average of grain size.

It is clear that E_B increases with increasing Co concentration, ranging from 71 to 446.5 V/mm. This means that E_B ranging from 92.2 to 292.5 V/mm increases with decreasing of the grain size of starting powders. The increase of E_B , in both cases, can be explained by the increase of the number of grain boundaries due to the decrease of the grain size average.

Conclusion

Nanopowders of pure ZnO and doped with (0–7 %) mol% Co have been synthesized by the sol–gel route to understand the origin of the varistor effect on this type of nanopowders.

To achieve this goal, powders with grain size below 100 nm were prepared.

The addition of Co up to 7 mol% did not affect the well-known peaks related to würtzite structure of ZnO.

This study permitted us to confirm that the grain size decreases by increasing of the Co concentration and increases by increasing of the calcination temperature.

The use of microwave sintering process allowed us to manufacture varistors with good quality (low density and efficient electrical properties).

The present investigation has also demonstrated that the non-linear coefficient increases by increasing of Co content and grain size.

The great merit of this method remains, undoubtedly, its velocity and the obtaining of ZnO–Co varistors with nano-sized grains.

Open Access This article is distributed under the terms of the Creative Commons Attribution License which permits any use, distribution, and reproduction in any medium, provided the original author(s) and the source are credited.

References

- Ait Ahcen T (2006) Doctorate Thesis, Algeria, 2006
- Anas S, Metz R, Sanoj MA, Mangalaraja RV, Ananthakumar S (2010) Sintering of surfactant modified ZnO–Bi₂O₃ based varistor nanopowders. *Ceram Int* 36:2351–2358
- Anas S, Metz R, Sanoj MA, Mangalaraja RV, Ananthakumar S (2012) Sintering of surfactant modified ZnO–Bi₂O₃ based varistor nanopowders. *Ceram Int* 38S:S457–S461
- Arab L, Hamdelou S, Harouni S, Guergouri K, Guerbous L (2012) Structural and luminescence properties of pure and Al-doped ZnO nanopowders. *Mater Sci Eng, B* 177:902–907
- Blatter G, Greuter F (1986) Carrier transport through grain boundaries in semi-conductors, *Phys Rev B* 33(6):3952–3966
- Cheng LH, Zheng LY, Meng L, Li GR, Gu Y, Zhang FP, Chu RQ, Xu ZJ (2012) Electrical properties of Al₂O₃-doped ZnO varistors prepared by sol–gel process for device miniaturization. *Ceram Int* 38S:S457–S461
- Duran P, Tartaj J, Moure C (2003) Fully dense, fine-grained, doped zinc oxide varistors with improved nonlinear properties by thermal processing optimization. *Journal of American Ceramic Society* 86:1326–1329
- Hembram K, Sivaprahasam D, Rao TN (2011) Combustion synthesis of doped nanocrystalline ZnO powders for varistors applications. *J Eur Ceram Soc* 31:1905–1913
- Levinson LM, Philipp HR (1975) The physics of metal oxide varistors. *Appl. Phys.* 46:1332
- Lin CC, Lee WS, Sun CC, Whu WH (2007) The influences of bismuth antimony additives and cobalt manganese dopants on the electrical properties of ZnO-based varistors. *Compos B* 38:338–344
- Long W, Hu J, Liu J, He J (2010) Effects of cobalt doping on the electrical characteristics of Al-doped ZnO varistors. *Mater Lett* 64:1081–1084
- Matsuoka M, Masuyama T, Iida Y (1969) Voltage nonlinearity of zinc oxide ceramics doped with alkali-earth metal oxide. *Jpn J Appl Phys* 8:1275–1276
- Miao WF, Ding J, McCormick PG, Street R (1996) A comparative study of mechanically alloyed and mechanically milled Nd₁₀Fe₈₄B₆. *J Appl Phys* 79:2079–2083
- Mirzayi M, Hekmatshoar MH (2013) Effect of V₂O₅ on electrical and microstructural properties of ZnO ceramics. *Phys B* 414:50–55
- Monteiro T, Boemare C, Soares MJ, Rita E, Alves E (2003) Photoluminescence and damage recovery studies in Fe-implanted ZnO single crystals. *J Appl Phys* 93:8995–9000
- Nahm CW (2003) Microstructure and electrical properties of Y₂O₃-doped ZnO–r₆O₁₁-based varistor ceramics. *Mater Lett* 57:1317–1321
- Nahm CW (2012) Nb₂O₅ doping effect on electrical properties of ZnO–V₂O₅–Mn₃O₄ varistor ceramics. *Ceram Int* 38:5281–5285
- Nahm CW, Kim HS (2002) Effect of Pr₆O₁₁/CoO mole ratio on nonlinear properties and DC accelerated aging characteristics of ZnO–Pr₆O₁₁–CoO–Dy₂O₃-based varistors. *Mater Lett* 56:379–385

- Nahm CW, Park JA, Shin BC, Kim IS (2004) Electrical properties and DC-accelerated aging behavior of ZnO–Pr₆O₁₁–CoO–Cr₂O₃–Dy₂O₃-based varistor ceramics. *Ceram Int* 30:1009–1016
- Onreabroy W, Sirikulrat N (2006) Effects of cobalt doping on nonlinearity of zinc oxide. *Mater Sci Eng, B* 130:108–113
- Onreabroy W, Sirikulrat N, Brown AP, Hammond C, Milne SJ (2006) Properties and intergranular phase analysis of a ZnO–CoO–Bi₂O₃ varistor. *Solid State Ionics* 177:411–420
- Peng Z, Fu X, Zang Y, Fu Z, Wang C, Qi L, Miao H (2010) Influence of Fe₂O₃ doping on microstructural and electrical properties of ZnO–Pr₆O₁₁ based varistor ceramic materials. *J Alloy Compd* 508:494–499
- Subasri R, Asha M, Hembram K, Rao GVN, Rao TN (2009) Microwave sintering of doped nanocrystalline ZnO and characterization for varistor applications, *Journal of Materials Chemistry and Physics* 115 (2009) 677–684
- Savary E, Marinel S, Gascoin F, Kinemuchi Y, Pansiot J, Retoux R (2011a) Peculiar effects of microwave sintering on ZnO based varistors properties. *J Alloy Compd* 509:6163–6169
- Savary E, Marinel S, Colder H, Harnois C, Lefevre FX, Retoux R (2011b) Microwave sintering of nano-sized ZnO synthesized by a liquid route. *Powder Technol* 208:521–525
- Sedky A, El-Brolossy TA, Mohamed SB (2012) Correlation between sintering temperature and properties of ZnO ceramic varistors. *J Phys Chem Solids* 73:505–510
- Subasri R, Asha M, Hembram K, Rao GVN, Rao TN (2009) Microwave sintering of doped nanocrystalline ZnO and characterization for varistor applications. *Mater Chem Phys* 115:677–684
- Wood VE, Austin AE (1975) *Magnetoelectric Interaction Phenomena in Crystals*. Gordon and Breach, London
- Wurst JC, Nelson JA (1972) Lineal intercept technique for measuring grain size in two-phase polycrystalline ceramics. *Journal of American Ceramic Society* 55:109–111